BIOMOLECULES & THERAPEUTICS

Original Article
Biomol Ther 28(5), 443-455 (2020)

Auranofin Enhances Sulforaphane-Mediated Apoptosis in Hepatocellular Carcinoma Hep3B Cells through Inactivation of the PI3K/Akt Signaling Pathway

Hyun Hwangbo[1,2], So Young Kim[1,2], Hyesook Lee[2], Shin-Hyung Park[3], Su Hyun Hong[4], Cheol Park[5], Gi-Young Kim[6], Sun-Hee Leem[7], Jin Won Hyun[8], Jaehun Cheong[1,*] and Yung Hyun Choi[2,4,*]

[1]Department of Molecular Biology, College of Natural Sciences, Pusan National University, Busan 46241,
[2]Anti-Aging Research Center, Dong-eui University, Busan 47340,
[3]Department of Pathology, Dong-eui University College of Korean Medicine, Busan 47227,
[4]Department of Biochemistry, Dong-eui University College of Korean Medicine, Busan 47227,
[5]Division of Basic Sciences, College of Liberal Studies, Dong-eui University, Busan 47340,
[6]Department of Marine Life Sciences, School of Marine Biomedical Sciences, Jeju National University, Jeju 63243,
[7]Department of Biological Science, College of Natural Sciences, Dong-A University, Busan 49315,
[8]Jeju National University School of Medicine and Jeju Research Center for Natural Medicine, Jeju 63243, Republic of Korea

Abstract

The thioredoxin (Trx) system plays critical roles in regulating intracellular redox levels and defending organisms against oxidative stress. Recent studies indicated that Trx reductase (TrxR) was overexpressed in various types of human cancer cells indicating that the Trx-TrxR system may be a potential target for anti-cancer drug development. This study investigated the synergistic effect of auranofin, a TrxR-specific inhibitor, on sulforaphane-mediated apoptotic cell death using Hep3B cells. The results showed that sulforaphane significantly enhanced auranofin-induced apoptosis by inhibiting TrxR activity and cell proliferation compared to either single treatment. The synergistic effect of sulforaphane and auranofin on apoptosis was evidenced by an increased annexin-V-positive cells and Sub-G1 cells. The induction of apoptosis by the combined treatment caused the loss of mitochondrial membrane potential ($\Delta\Psi m$) and upregulation of Bax. In addition, the proteolytic activities of caspases (-3, -8, and -9) and the degradation of poly (ADP-ribose) polymerase, a substrate protein of activated caspase-3, were also higher in the combined treatment. Moreover, combined treatment induced excessive generation of reactive oxygen species (ROS). However, treatment with N-acetyl-L-cysteine, a ROS scavenger, reduced combined treatment-induced ROS production and apoptosis. Thereby, these results deduce that ROS played a pivotal role in apoptosis induced by auranofin and sulforaphane. Furthermore, apoptosis induced by auranofin and sulforaphane was significantly increased through inhibition of the phosphoinositide 3-kinase (PI3K)/Akt pathway. Taken together, the present study demonstrated that down-regulation of TrxR activity contributed to the synergistic effect of auranofin and sulforaphane on apoptosis through ROS production and inhibition of PI3K/Akt signaling pathway.

Key Words: Auranofin, Sulforaphane, TrxR, Apoptosis, ROS, PI3K/Akt

INTRODUCTION

The incidence of liver cancer including hepatocellular carcinoma (HCC) is the sixth most common incidence of cancer and ranks third among the cancer deaths worldwide (Ferlay *et al*., 2018). While most cases of HCC are caused by infection with hepatitis B or C virus (HBV or HCV) or excessive alcohol consumption, recent studies predicted that increases in the number of cases of non-alcoholic fatty liver (NAFLD), which increased the risk of HCC, along with metabolic syndrome and obesity, will sooner or later become a major cause of HCC (Baffy *et al*., 2012; Kulik and El-Serag, 2019). Current options for the treatment of HCC are radiation therapy, surgical resection, and chemotherapy for advanced-stage HCC (Llovet *et*

Open Access **https://doi.org/10.4062/biomolther.2020.122**

Received Jul 9, 2020 **Revised** Jul 22, 2020 **Accepted** Jul 22, 2020
Published Online Sep 1, 2020

***Corresponding Authors**
E-mail: molecule85@pusan.ac.kr (Cheong J), choiyh@deu.ac.kr (Choi YH)
Tel: +82-51-510-2277 (Cheong J), +82-51-890-3319 (Choi YH)
Fax: +82-51-513-9258 (Cheong J), +82-51-890-3333 (Choi YH)

al., 2018; Likhitsup et al., 2019). However, no treatment has shown remarkable results in treating HCC due to side effects, treatment inefficiency, drug toxicity, and resistance and insufficient anticancer effects. Yet, chemotherapy is still the main treatment for HCC (Conklin, 2000; Trotti et al., 2000; Schirrmacher, 2019). Therefore, it is imperative to identify therapeutic agents for HCC with low toxicity and high effectiveness.

The thioredoxin (Trx) and Trx reductase (TrxR) system is composed of Trx and nicotinamide adenine dinucleotide phosphate (NADPH)-dependent TrxR, which is functionally involved in several processes including anti-oxidation, redox regulation and cell proliferation (Arnér and Holmgren, 2000; Lu and Holmgren, 2014). Several previous studies reported that Trx or TrxR was overexpressed in acute lymphocytic leukemia, lung, breast, colorectal, pancreatic, hepatocellular and gastric cancers, and the sensitivity to radiotherapy and chemotherapy in the treatment of melanoma, colon, and breast cancer was further increased by TrxR suppression (Lincoln et al., 2003; Urig and Becker, 2006). TrxR has a redox-active center consisting of a cysteine-selenocysteine redox pair, and the metal complex can be bound to the active site to inhibit its activity (Zhong et al., 2000; Ren et al., 2018). Consequently, TrxR is expected to be a pharmacological target for metallodrugs (Becker et al., 2000; Cheng and Qi, 2017).

Auranofin is a gold phosphine complex and has been used as a medication for rheumatoid arthritis, but is more recently known as a TrxR inhibitor (Isab and Shaw, 1990; Madeira et al., 2012). Auranofin can inactivate TrxR by forming diselenide bridges with the human TrxR Sec 498 residue, reducing the NADPH-dependent reduction of oxidized thioredoxin and thus, affecting intracellular redox regulation, cell proliferation and antioxidant defense (Becker et al., 2000; Fang and Holmgren, 2006). Auranofin induces apoptosis of tumor cells and excessive reactive oxygen species (ROS) production by modulating the cellular redox status (Marzano et al., 2007; Cox et al., 2008). Based on evidence that TrxR inhibition and ROS accumulation inhibited cancer cell growth, auranofin has been considered for an anti-cancer agent for leukemia, lung cancer and epithelial ovarian cancer (Madeira et al., 2012; Ralph et al., 2019; U.S. National Library of Medicine, ClinicalTrials.gov).

Phytochemicals, natural plant-derived bioactive components, are helpful compounds with few side effects and a variety of potential roles as chemical and biological functional agent (Phan et al., 2018). One of the phytochemicals, sulforaphane (1-isothiocyanato-4-(methanesulfinyl)-butane) is an isothiocyanate, which is abundant in cruciferous vegetables such as broccoli, cabbage and cauliflower (Robbins et al., 2005). Sulforaphane has reported anti-cancer effects through cell cycle arrest and apoptosis in various cancer cells, such as prostate, lung, breast, and colon cancers (Gamet-Payrastre et al., 2000; Herman-Antosiewicz et al., 2006; Mi et al., 2007; Li et al., 2010). Although our previous studies confirmed the anticancer effects of sulforaphane or auranofin in Hep3B cells (Moon et al., 2010; Hwang-Bo et al., 2017), the combined treatment of sulforaphane with auranofin has not been evaluated. In the present study, sulforaphane and auranofin were used to evaluate the synergistic effect of combination therapy on apoptosis to effectively increase anti-cancer activity in Hep3B cells.

MATERIALS AND METHODS

Materials

Auranofin, sulforaphane, N-acetyl-L-cysteine (NAC), collagenase from Clostridium histolyticum, tetraethylbenzimidazolylcarbocyanine iodide (JC-1) dye, 4′,6-diamidine-2′-phenylindole dihydrochloride (DAPI) and 2',7'-dichlorodihydrofluorescein diacetate (DCFH-DA) were purchased from Sigma-Aldrich Chemical Co (St. Louis, MO, USA). Fetal bovine serum (FBS), Dulbecco's modified Eagle medium (DMEM), penicillin-streptomycin and trypsin ethylenediaminetetraacetic acid (EDTA) were obtained from WELGENE Inc (Daegu, Korea). Cell culture products were purchased from SPL (Houston, TX, USA). Williams E medium, no phenol red, was purchased from GIBCO BRL (Grand Island, NY, USA). 3-(4,5-dimethylthiazol-2-yl)-2,5-diphenyltetrazolium bromide (MTT) and Mitotracker were purchased from Invitrogen (Waltham, MA, USA). Dimethyl sulfoxide (DMSO) was purchased from Amresco Inc (Solon, OH, USA). The Cycletest Plus DNA reagent kit, propidium iodide (PI) solution, and fluorescein isothiocyanate-conjugated (FITC) annexin-V were purchased from BD Pharmingen (San Diego, CA, USA). Protein assay dye and Laemmli sample buffer were obtained from Bio-Rad Laboratories, Inc (Hercules, CA, USA). Primary hepatocyte maintenance supplements, electrochemiluminescence (ECL) reagent, mitochondrial superoxide indicator (MitoSOX) were purchased from Thermo Fisher Scientific (Waltham, MA, USA). Nitrocellulose membranes were purchased from GE Healthcare (Chicago, IL, USA). Anti-poly (ADP-ribose) polymerase (PARP, 1:1,000, sc-7150), X-linked inhibitor of apoptosis protein (XIAP, 1:1,000, sc-11426), cellular inhibitor of apoptosis protein (cIAP-1, 1:1,000, sc-7943), Bcl-2 (1:1,000, sc-783), Bax (1:1,000, sc-493), Bid (1:1,000, sc-11423), Akt (1:1,000, sc-8312), phosphorylated Akt (p-Akt, 1:1,000, sc-101629), and secondary antibodies were obtained from Santa Cruz Biotechnology (Dallas, TX, USA). Anti-phosphoinositide 3-kinase (PI3K, 1:1,000, 4292S) and phosphorylated PI3K (p-PI3K, 1:1,000, 4228S) were purchased from Cell Signaling Technology (Danvers, MA, USA).

Cell culture and chemicals

HCC Hep3B and HepG2 cells were obtained from the American Type Culture Collection (Manassas, VA, USA). The cells were cultured in DMEM medium supplemented with 10% (v/v) FBS and 1% penicillin/streptomycin and incubated in a humidified atmosphere containing 5% CO_2 at 37°C. Auranofin and sulforaphane were dissolved in DMSO with stock concentrations of 10 mM and 20 mM, respectively, and stored at –20°C until use. The culture media used for cell treatment contained a final concentration of DMSO of up to 0.04% or less, it is concentration in which cytotoxicity does not appeared.

Primary hepatocytes isolation

Primary hepatocytes were isolated from 6-week-old male C57BL/6 mice and used immediately after hepatic portal perfusion and isolation, as previously described (Hwang-Bo et al., 2019). In brief, the portal vein of the liver was continuously injected with ethylene glycol-bis(2-aminoethylether)-N,N,N′,N′-tetraacetic acid (EGTA) buffer (5.4 mM KCl, 0.44 mM KH_2PO_4, 140 mM NaCl, 0.34 mM Na_2HPO_4, 0.5 mM EGTA, and 25 mM Tricine) at a rate of 5 mL/min, and the injected buffer and blood were discharged by cutting the infrahepatic inferior vena cava. To disperse the liver tissue, 0.075% collagenase was addi-

Table 1. The binding information of auranofin-TrxR1 and sulforaphane-TrxR1 complex

Molecule	PDB ID	Ligand	Pubchem ID	Binding affinity (kcal/mol)	Binding site
Thioredoxin reductase	2ZZ0	Auranofin	CID 70788951	–5.5	O (Cys 498)
		Sulforaphane	CID 24724618	–3.6	O (Asp 334)

tionally perfused. The digested liver tissue was washed and filtered with a 40 μm cell strainer. The hepatocyte pellets were collected and a Percoll cushion (45%) was used to perform gradient-based hepatocyte isolation. The cells were cultured in Williams E medium with no phenol red supplemented with primary hepatocyte maintenance supplements and incubated overnight at 37°C in 5% CO_2.

Cell viability assay

To investigate cell viability, the cells were seeded in 6-well plates at 1.5×10^5 cells per well and incubated at 37°C for 24 h. The cells were treated with auranofin (0.5, 1, 1.5, and 2 μM) or sulforaphane (2.5, 5, 7.5, and 10 μM) for 24 h, and then 200 μL of MTT at 5 mg/mL was added, as previously described (Hasan *et al*., 2019). After 2 h, the medium was removed and 2 mL of DMSO was added to each well for 10 min. The cell viability was measured by an enzyme-linked immunosorbent assay (ELISA) reader (Molecular Devices, Sunnyvale, CA, USA) at 540 nm. The results are expressed as percentages of the treated group compared to the control group.

TrxR enzymatic activity assay

TrxR activity was measured by utilizing a TrxR colorimetric assay kit (Cayman Chemical, Ann Arbor, MI, USA), based on the NADPH-dependent reduction of 5, 5'-dithio-bis-(2-nitrobenzoic) acid (DTNB) to 5-thio-2-nitrobenzoic acid. In brief, cells were seeded in a 100 mm dish at a plating density of 7.5×10^5 cells/dish and treated with the indicated concentration of auranofin and sulforaphane for 24 h. After that, the cells were harvested and homogenized in a buffer containing 50 mM potassium phosphate, pH 7.4 and 1 mM EDTA. The samples (20 μL) were added to 96-well plates, and then 180 μL of the reaction mix (140 μL assay buffer, 20 μL DTNB and 20 μL NADPH) was added. The linear increase in absorbance at 412 nm was measured during 15 min using ELISA plate reader. TrxR activity was calculated as a percentage of the enzyme activity compared to that of the control group.

Flow cytometry analysis of apoptosis

To determine apoptotic cell death, the ratio of sub-G1 and annexin-V-positive cells were analyzed by flow cytometry according to the previously described method (Zhang *et al*., 2020). The cells were seeded and stabilized on a 6-well plate (1.5×10^5 cells/well), and then incubated with the indicated concentrations of auranofin and sulforaphane for 24 h. To measure the sub-G1 DNA population and apoptotic cell death, the cells were stained by PI solution and FITC annexin-V, respectively, and analyzed with an Accuri C6 flow cytometer (BD Sciences, Franklin Lakes, NJ, USA) at Core-Facility Center for Tissue Regeneration, Dong-eui University (Busan, Korea). For each experiment, 10,000 events per sample were recorded.

Caspase-3, -8 and -9 activity

To quantify caspase activity, the cells were seeded in 100 mm dishes at 7.5×10^5 cells and stabilized for 24 h. The cells were exposed with or without 1 μM of auranofin and the indicated concentration of sulforaphane for 24 h. Caspase activities were determined using caspase-3, -8 and -9 colorimetric assay kits (R&D Systems, Minneapolis, MN, USA) performed according to the manufacturer's protocol. After the treatment period, the cells were harvested and lysed with lysis buffer, and the protein content was quantitated at 3 μg/μL. Cell lysates (50 μL) were dispensed into each reaction well, and 2×reaction buffer (50 μL), and DEVD (Asp-Glu-Val-Asp), IETD (Ile-Glu-Thr-Asp), and LEHD (Leu-Glu-His-Asp), which were substrate of caspase-3, -8 and -9, respectively, were added and incubated at 37°C for 1-2 h. The samples were assessed with a ELISA reader (Molecular Devices) at a wavelength of 405 nm.

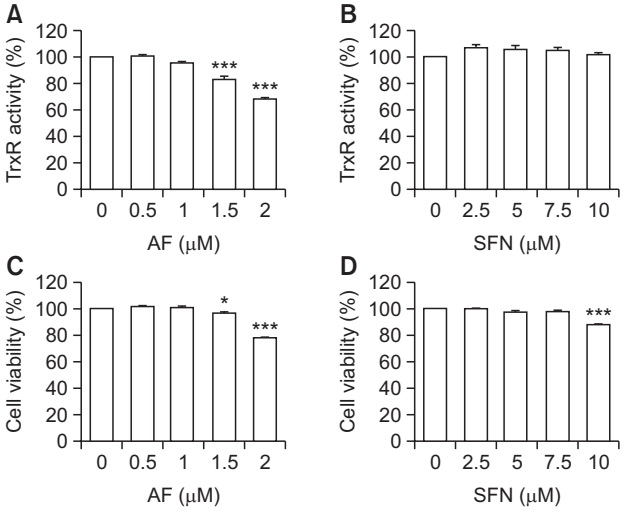

Fig. 1. Effects of auranofin and sulforaphane on TrxR activity and cell viability in Hep3B cells. Hep3B cells were treated with the indicated concentrations of auranofin (AF) or sulforaphane (SFN) for 24 h. (A, B) The cells were harvested and lysed to measure TrxR1 activity using a colorimetric assay kit. Absorbance was measured using a ELISA reader (Molecular Devices, Sunnyvale, CA, USA) and calculated as described by the manufacturer's protocol. (C, D) MTT assay was performed to confirm the cell viability affected by auranofin and sulforaphane. The absorbance was measured using a ELISA reader (Molecular Devices), and the results were compared by setting the control group viability to 100%. The data represent the average of three independent experiments (mean ± SD). Statistical analysis was performed using ANOVA with Tukey's post-hoc test (*p<0.05, ***p<0.001).

Western blot analysis

The cells were treated with or without 1 μM of auranofin and the indicated concentration of sulforaphane for 24 h and then the cells were harvested, washed in phosphate-buffered saline (PBS), and lysed in lysis buffer [250 mM NaCl, 25 mM Tris-Cl

(pH 7.5), 5 mM EDTA (pH 8.0), 1% NP-40, 1 mM 4-(2-aminoethyl) benzenesulfonyl fluoride hydrochloride, 5 mM dithiothreitol, and protease inhibitor cocktail] followed by centrifugation at 14,000 rpm for 30 min at 4°C. The supernatants were collected and the protein concentrations were estimated with a ELISA reader (Molecular Devices) at 595 nm using a protein assay dye. After quantification at 3 μg/ul protein per sample and mixing 1:1 with Laemmli sample buffer, the samples were heated at 95°C for 5 min to denature the protein and stored at –80°C until use. To perform sodium dodecyl sulfate-polyacrylamide gel electrophoresis (SDS-PAGE), 15 μg of protein sample was loaded in each lane of 12% SDS-polyacrylamide gels, electrophoresed, and transferred to membranes. The membranes were blocked with 5% skim milk in PBS containing 0.1% Tween 20 (PBST) for 1 h and then, probed with the appropriate concentrations of primary antibodies overnight at 4°C. After washing three times with PBST, the membranes were reacted with secondary antibody (anti-mouse or anti-rabbit) for 2 h at room temperature, and the proteins were visualized using ECL.

Evaluation of mitochondrial membrane potential (MMP)

JC-1 dye, as an MMP (*Δψm*) indicator, can selectively enter mitochondria and reversibly change color from red fluorescence to green fluorescence with decreases in MMP. In healthy cells with high MMP, JC-1 is present as an aggregate that exhibits red, and has a monomeric form that is green in apoptosis-induced cells. After auranofin and sulforaphane administration, the cells were harvested and stained with 10 μg/mL JC-1 for 20 min in the dark. The MMP changes by treatment were analyzed by Accuri C6 flow cytometer and fluorescence imaging system (EVOS FL Auto 2, Thermo Fisher Scientific).

Detection of intracellular ROS and mitochondrial superoxide

In brief, the cells were pre-treated with NAC for 1 h and then further incubated with auranofin (1 μM) and sulforaphane (7.5 μM) for 1 h. After the incubation, the cells were exposed to DCFH-DA (10 μM) and MitoSOX (10 μM) for 20 min at 37°C. Then, the cells were harvested and the intracellular ROS levels were measured using flow cytometry. The samples were further stained with DAPI and Mitotracker and visualized us-

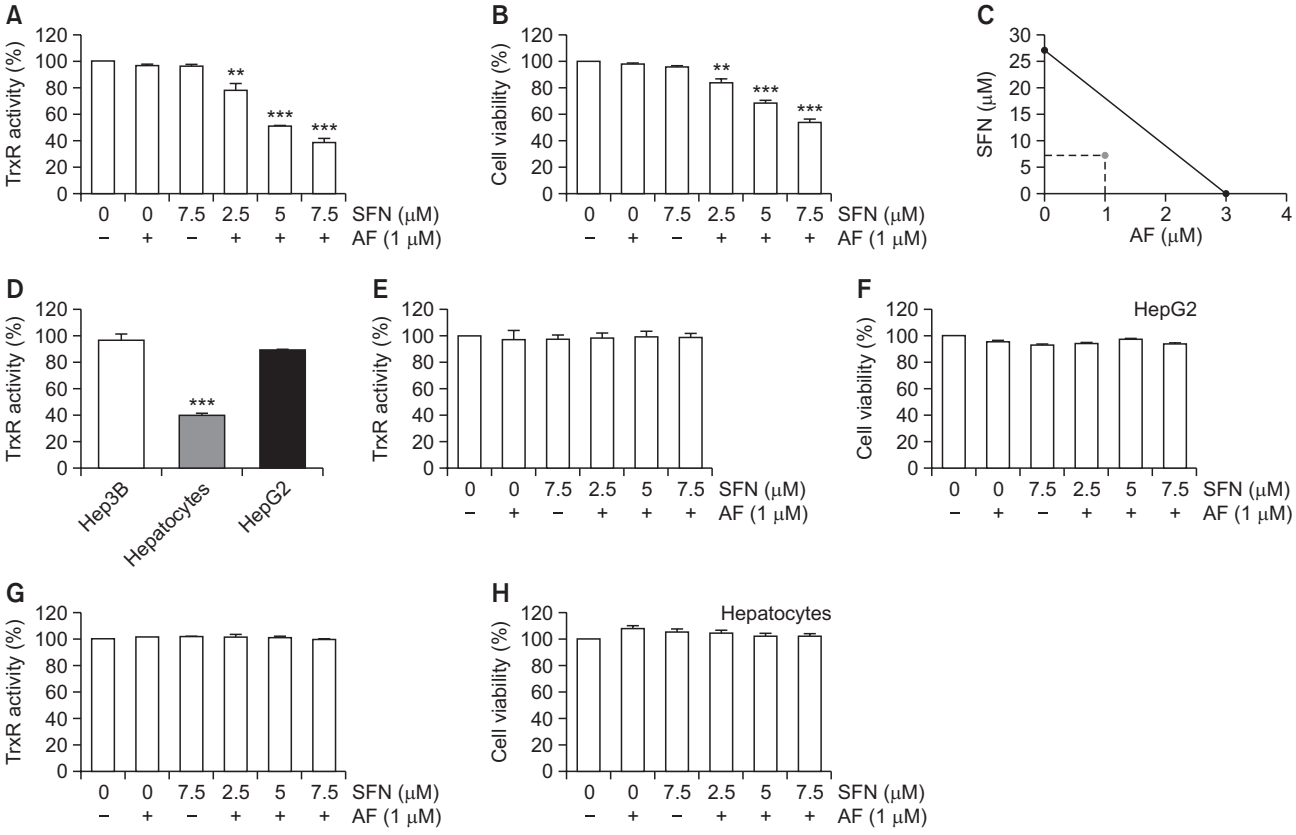

Fig. 2. Synergistic effects of auranofin (AF) and sulforaphane (SFN) on the inhibition of TrxR1 activity and cell viability in Hep3B cells. Hep3B, HepG2 cells and primary hepatocytes were incubated with auranofin and sulforaphane alone or together for 24 h. (A, D, E, G) Cellular TrxR activity was measured *in vitro* using an DTNB assay. (B, F, H) Cell viability was determined by an MTT assay. The absorbance was measured using an ELISA plate reader and compared to the control which was set to 100%. The data are the average of three independent experiments (mean ± SD). Statistical analysis was performed using one-way ANOVA with Tukey's post-hoc test (***p*<0.01 and ****p*<0.001). (C) The isobologram analysis for the synergism of auranofin and sulforaphane was drawn based on the half maximal inhibitory concentration (IC_{50}). The straight lines connecting the respective IC_{50} values for the two agents correspond to the effects independent of each other, and the values below the straight lines indicate the synergistic effects.

ing a fluorescence imaging system (EVOS FL Auto 2, Thermo Fisher Scientific).

Molecular docking

The molecular docking of the enzyme-compound complexes was calculated (tested, performed, conducted) by their binding affinity and binding sites using a PyRx virtual screening program (https://pyrx.sourceforge.io). The 3D structure of TrxR was acquired from the Protein Data Bank (PDB). Its PDB ID code was 2CFY. Additionally, the two-dimensional structure of auranofin and sulforaphane were obtained from The National Center for Biotechnology Information (NCBI) PubChem compound database. Each compound ID (CID) is shown in Table 1. The virtual screening results from Pyrx were analyzed and expressed with PyMOL (https://pymol.org).

Statistical analysis

All statistical analyses were performed with GraphPad Prism (GraphPad Software, Inc., La Jolla, CA, USA) using one-way analysis of variance (ANOVA) for multiple compari-

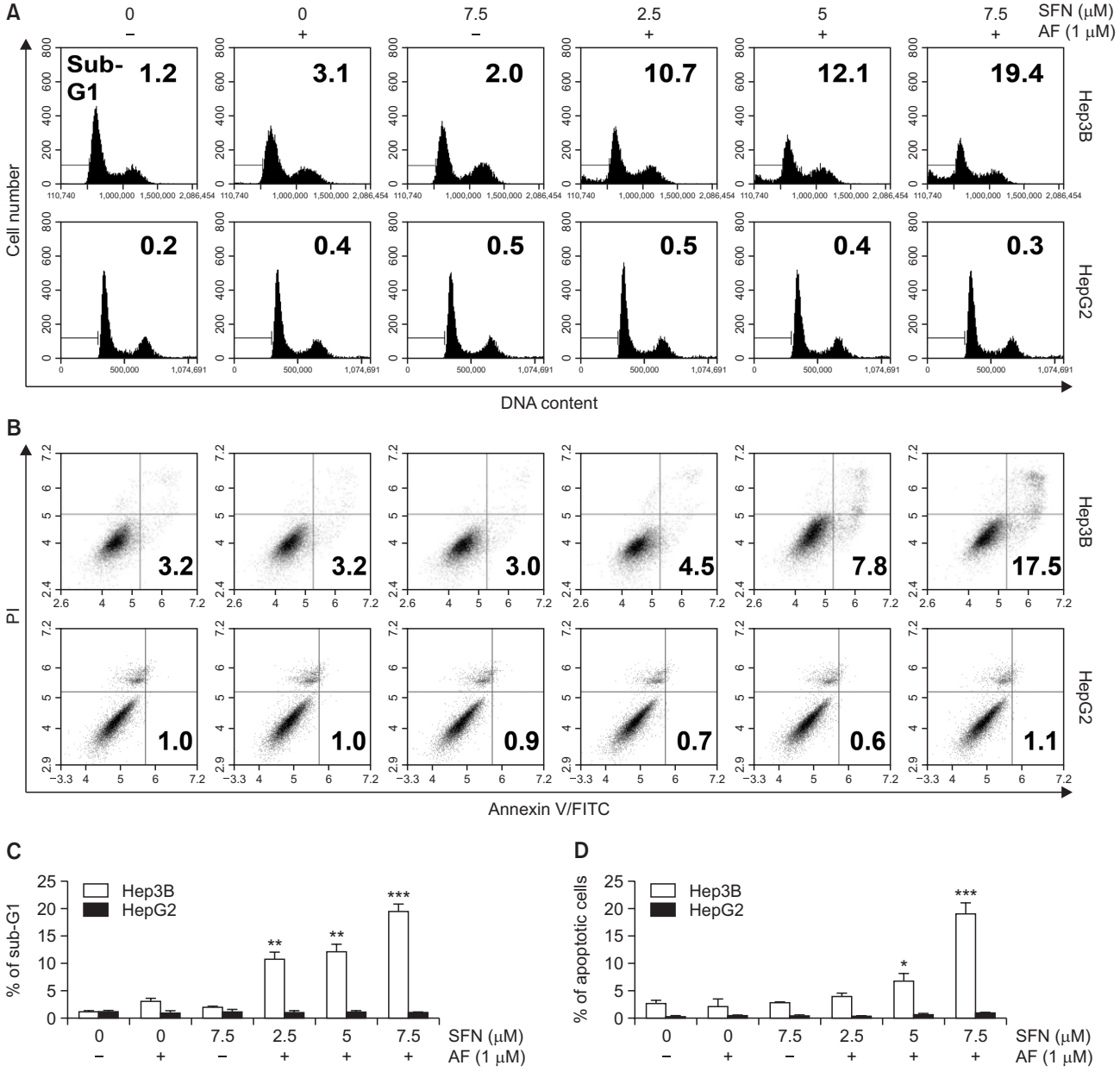

Fig. 3. Induction of apoptosis by combined treatment with auranofin (AF) and sulforaphane (SFN) in Hep3B cells. Hep3B and HepG2 cells were exposed to auranofin and sulforaphane at the indicated concentrations for 24 h. Cell cycle analysis (A, C) and apoptotic cell death (B, D) were quantified for auranofin and sulforaphane treated-Hep3B and HepG2 cells using flow cytometry and shown by histograms and dot plot diagrams. The results were obtained from three independent experiments. The figures are representative of one of the experimental results. Statistical analysis was performed using one-way ANOVA with Tukey's post-hoc test (*p<0.05, **p<0.01, and ***p<0.001).

sons, followed by Tukey's post hoc test. Each experiment was evaluated at least three times, and all numerical data are expressed as means ± standard deviation (SD). Results with a p value<0.05 were considered statistically significant.

RESULTS

Synergistic suppression of TrxR1 activity and cell viability by auranofin and sulforaphane in Hep3B cells

As shown in Fig. 1, treatment with either sulforaphane or auranofin alone at low concentrations weakly inhibit TrxR activity and decreased cell viability in Hep3B cells. After confirming the auranofin and sulforaphane conditions that did not affect Hep3B cells, combined treatment was performed to measure TrxR activity and cell viability. Combined treatment significantly reduced TrxR activity and cell viability compared to single treatments with auranofin or sulforaphane in Hep3B cells (Fig. 2A, 2B). Next, the synergistic effect of auranofin and sulforaphane on growth inhibition was quantified by isobologram analysis (Fig. 2C). The difference in basal TrxR activity in the two types of HCCs (Hep3B and HepG2 cells) and normal hepatocytes without chemical treatment was measured. As shown in Fig. 2D, TrxR activity in HCCs was higher than normal hepatocytes. However, combined treatment did not alter the TrxR activity and cell viability in HepG2 and normal hepatocytes (Fig. 2E-2H).

Sulforaphane has synergistic effects with auranofin on the induction of apoptosis and activity of caspases in Hep3B cells

Apoptosis was quantified and visualized in various ways to determine whether the cell viability reduced by the combined treatment was due to apoptosis. In the first method of quantifying apoptosis, the percentage of sub-G1 cells was determined by measuring the cellular DNA content. The results showed that the percentage of sub-G1 cells was increased by auranofin and sulforaphane treatment (Fig. 3A, top, 3C). The annexin-V/PI-double staining, another method of quantification of apoptosis, also confirmed that apoptosis was increased by the combined treatment with auranofin and sulforaphane (Fig. 3B, top, 3D). However, auranofin and sulforaphane did not increase the number of sub-G1cells (Fig. 3A, bottom, 3C) and annexin-V-positive cells (Fig. 3B, bottom, 3D) in HepG2 cells. To determine which regulators affected the combined treatment-induced apoptosis, caspase activity assays and Western blot experiments were conducted. In the caspase activity assays, the combined treatment led to increased caspase-3 and -9 activity, whereas caspase-8 activity was not significantly changed (Fig. 4A). The results of Western blotting showed that the combined treatment increased cleavage of PARP, a downstream target of activated caspase-3, and decreased the expression of inhibitor of apoptosis protein (IAP) members including XIAP and cIAP-1 (Fig. 4B).

Loss of mitochondrial dysfunction in apoptosis induced auranofin and sulforaphane in Hep3B cells

The expression of Bax, a protein present in mitochondria and involved in apoptosis, increased, but there was no change in the expression of Bcl-2 and Bid (Fig. 4C). Therefore, the loss of MMP ($\Delta\psi m$), one of the events in apoptosis, was evaluated to determine whether the combined treatment affected mitochondrial function. As shown in Fig. 5, the JC-1 aggregates emit orange fluorescence at the control level, and JC-1 monomers emitted green fluorescence, specifically due to MMP loss, which was induced in Hep3B cells by the combined treatment but not in HepG2 cells. These results demonstrate that the combined treatment induced apoptosis and that the pathway proceeded via mitochondrial dysfunction.

Elevated cellular ROS and mitochondrial superoxide by combined treatment with auranofin and sulforaphane in Hep3B cells

To measure excess intracellular ROS, flow cytometry analysis and fluorescent images were observed using DCFH-DA, a cell penetrable ROS probe. As shown in Fig. 6A, after combined treatment for 1 h, the amount of ROS was increased by about 3-fold (9.6%) compared to the control group (3.1%). To confirm whether the generation of ROS caused by auranofin and sulforaphane mediated mitochondria, mitochondrial superoxide was measured by staining with MitoSOX. As with the DCFH-DA staining results, the percentage of mitochondrial superoxide increased with auranofin and sulforaphane treatment but was restored by NAC (Fig. 6B). Furthermore, the fluorescence emission of DCFH-DA (green) and Mitotracker mitochondrial (red) staining was observed under a fluorescent microscope to visually confirm these results. As shown in Fig. 6C, DCFH-DA, an ROS probe, was not only increased intracellularly but also co-localized with Mitotracker staining.

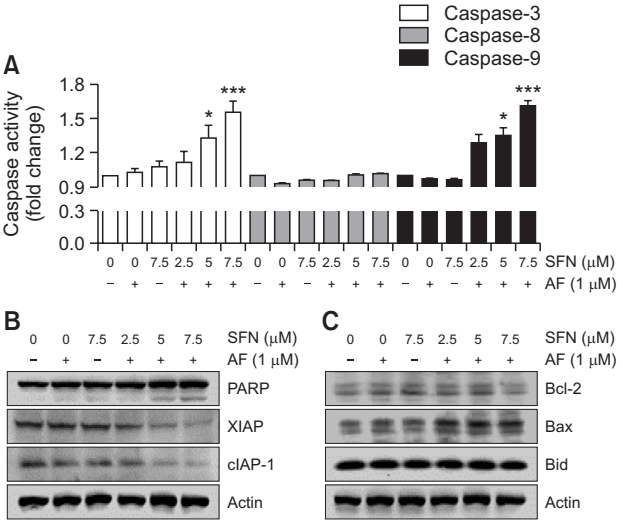

Fig. 4. Effects of combined treatment with auranofin (AF) and sulforaphane (SFN) on caspase activity and apoptosis-regulatory protein expression in Hep3B cells. The cells were incubated with 1 μM of auranofin and the indicated concentration of sulforaphane for 24 h. (A) Quantitative analysis of caspases-3, -8, and -9 activity *in vitro*. The cells were lysed and assayed for caspase-3, -8, and -9 activity using the appropriate substrates. The colorimetric assay was measured using a ELISA reader (Molecular Devices, Sunnyvale, CA, USA). All results represent three independent determinations with fold increases calculated based on the control group. *p<0.05 and ***p<0.001 compared to the control group. (B, C) The cells were lysed and equal amounts of cellular proteins were subjected to Western blotting analysis using specific primary antibodies corresponding to each protein. Equal protein loading was confirmed by actin expression.

Moreover, an ROS scavenger was used to confirm the association between the induction of apoptosis by auranofin plus sulforaphane and ROS production.

As shown in Fig. 7A and 7F, TrxR activity and cell viability inhibited by the combined treatment were restored to control levels by pretreatment with NAC. Likewise, the annexin-V-positive cells and loss of MMP (*Δψm*), which were increased by auranofin and sulforaphane, was decreased by NAC (Fig. 7C, 7D). Also, the expression of apoptosis-related proteins including PARP and XIAP were altered to control level (Fig. 7E). Considering that the induction of apoptosis and mitochondrial-mediated ROS by auranofin and sulforaphane was decreased by NAC, these results suggest that ROS production was responsible for the combined treatment-induced apoptosis. However, cell viability, apoptotic cell death and MMP loss were not altered in HepG2 cells by the combined treatment (Fig. 7B-7D, bottom).

Suppression of PI3K/AKT signaling pathway by auranofin and sulforaphane

To estimate whether sulforaphane and auranofin affected the PI3K/Akt pathway, the cells were treated with the combined treatment for varying incubation times (0.5, 1, 3, 6, 12, and 24 h). Western blotting was used to confirm the expression of phosphorylated PI3K/Akt. As shown in Fig. 8A, with increasing incubation times of combined treatment, the expression levels of p-PI3K and its downstream protein p-Akt decreased. Additionally, LY2940020, an inhibitor of PI3K/Akt signaling, was used to determine the effect of combined treatment-induced apoptosis. The results showed that pretreatment with PI3K/Akt inhibitor further decreased cell viability (Fig. 8C) and enhanced apoptotic cell death (Fig. 8B, top) and cleavage form of PARP (Fig. 8E) in Hep3B cells compared to the combined treatment without pretreatment. However, combined treatment and LY294002 did not change the cell viability and apoptosis in HepG2 cells (Fig. 8B, bottom, 8D).

Regulation of ROS-mediated PI3K/Akt signaling by auranofin and sulforaphane

Furthermore, whether ROS or PI3K/Akt pathway acted upstream in combined treatment-induced apoptosis was confirmed using ROS and PI3K/Akt inhibitors (NAC and LY294002, respectively). The cells were pretreated with NAC and LY294002 for 1 h and then incubated with auranofin plus sulforaphane for 24 h. After pretreatment with NAC/LY294002 and combined treatment, cell viability (Fig. 9A) and TrxR activity (Fig. 9F) were restored to control levels; annexin-V-positive cells (Fig. 9C, top), loss of MMP (Fig. 9D, top) and cleavage

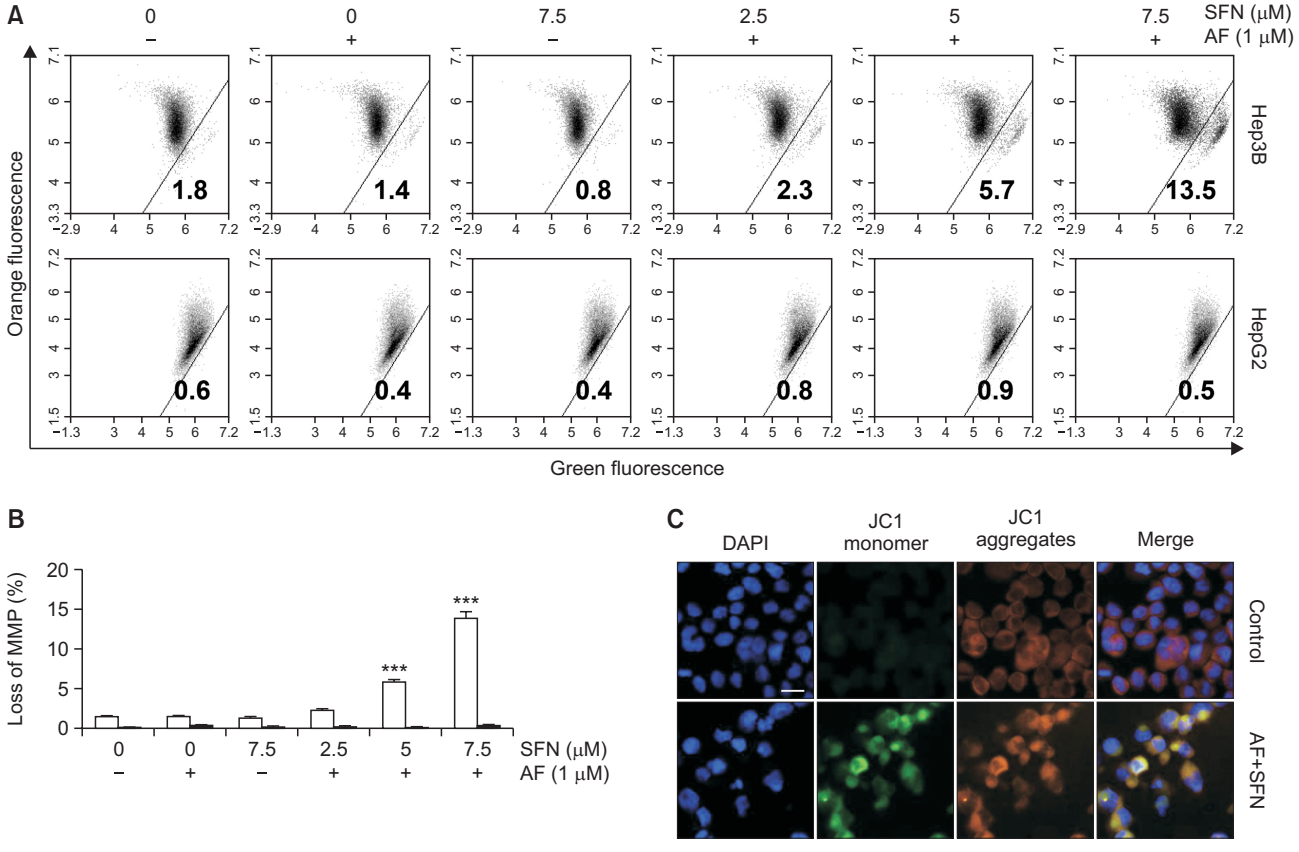

Fig. 5. Loss of MMP (*Δψm*) by the combined treatment of Hep3B cells. Hep3B and HepG2 cells were incubated with auranofin (AF) (1 μM) and sulforaphane (SFN) (2.5, 5 and 7.5 μM) for 24 h and then stained with JC-1 dye for 24 min to measure changes in MMP, quantitated by flow cytometry analysis (A, B), and observed with a fluorescence microscope (C). The increase in JC-1 monomer (green fluorescence) and decreases in JC-1 aggregates (orange fluorescence) in the JC-1 ratio (aggregates: monomer) indicated loss of MMP (*Δψm*). Scale bar=25 μm. The results were obtained from three independent experiments. Statistical analysis was performed using one-way ANOVA with Tukey's post-hoc test (***p<0.001).

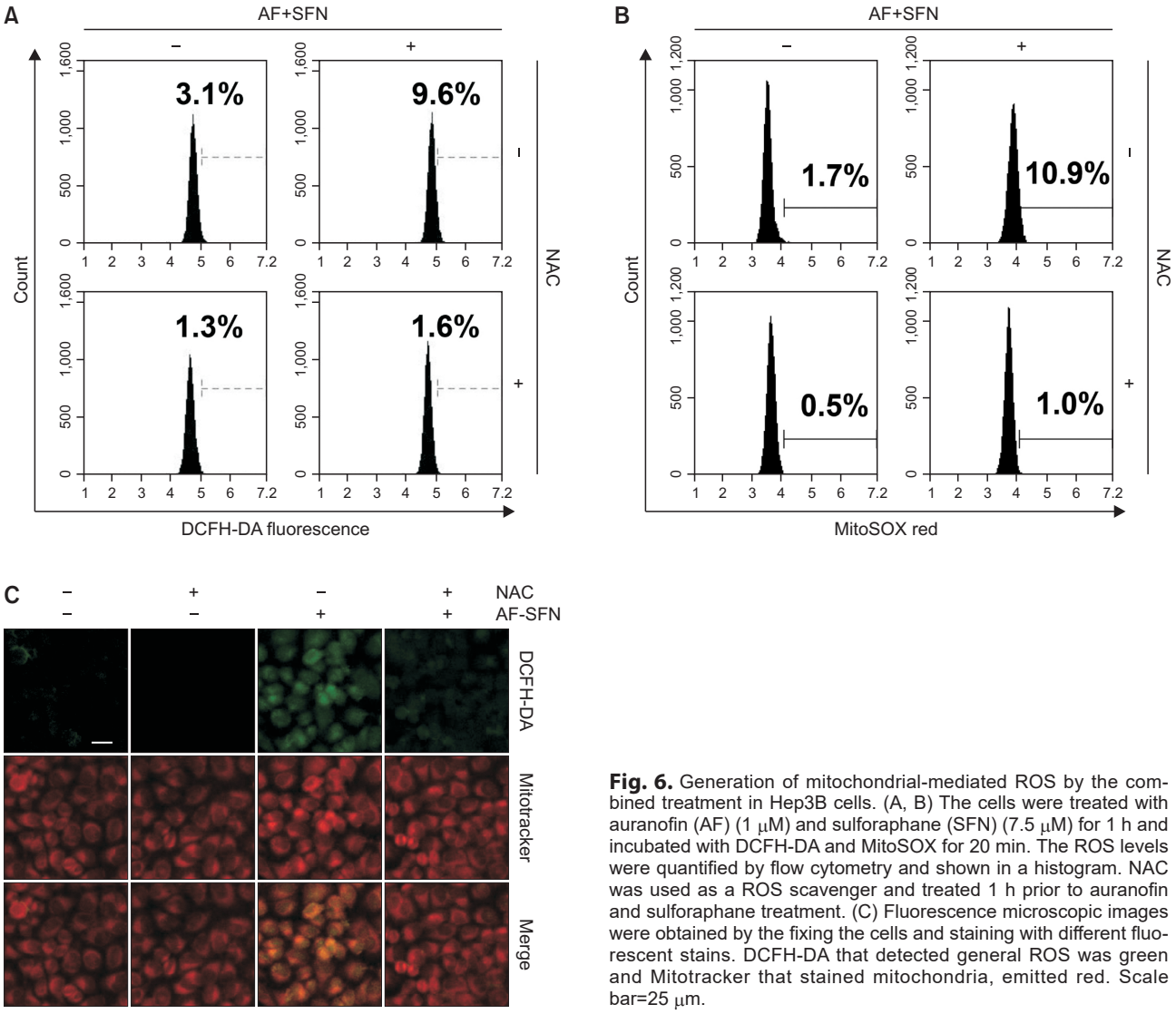

Fig. 6. Generation of mitochondrial-mediated ROS by the combined treatment in Hep3B cells. (A, B) The cells were treated with auranofin (AF) (1 μM) and sulforaphane (SFN) (7.5 μM) for 1 h and incubated with DCFH-DA and MitoSOX for 20 min. The ROS levels were quantified by flow cytometry and shown in a histogram. NAC was used as a ROS scavenger and treated 1 h prior to auranofin and sulforaphane treatment. (C) Fluorescence microscopic images were obtained by the fixing the cells and staining with different fluorescent stains. DCFH-DA that detected general ROS was green and Mitotracker that stained mitochondria, emitted red. Scale bar=25 μm.

form of PARP were reduced; and the expression of XIAP increased to the control levels (Fig. 9E) in Hep3B cells but not in HepG2 cells (Fig. 9B-9D, bottom). The above-mentioned results indicated that the combined treatment-induced apoptosis suppressed PI3K/Akt signaling via the ROS-dependent pathway.

Molecular modeling of auranofin and sulforaphane docking to TrxR1

To support the results that auranofin and sulforaphane inhibited TrxR activity, molecular modeling of the binding interaction of TrxR1 with auranofin and sulforaphane was conducted using PyRx (The Scripps Research Institute, CA, USA). The enzyme-compound complexes were analyzed for docking using PyRx (The Scripps Research Institute) and visualized by PyMOL (Schrodinger, Inc., NY, USA). As shown in Table 1 and Fig. 10, auranofin and sulforaphane were predicted to be covalently bound to TrxR1 and located in different surface pockets of TrxR1. Auranofin bound to TrxR1 with a high affinity (–5.5 kcal / mol) and interacted with the Cys 498 residue, which is essential for the catalytic activity of TrxR1 (Fig. 10C, 10D, left panel). To confirm the critical role of the Cys 498 residue in the TrxR1-auranofin complex, the Cys 498 residue was mutated to alanine (Ala), which eliminated the binding of TrxR1 to the essential residue of TrxR1 (Fig. 10C, 10D, right panel). Sulforaphane was predicted to interact covalently with the Asp 334 of TrxR1, which was not as strong as auranofin (Fig. 10C, 10D, middle panel). Therefore, these results demonstrated that TrxR and auranofin and sulforaphane interacted structurally and electrochemically.

DISCUSSION

Chemotherapy is associated with cytotoxicity, which leads to cell death not only of tumors but also of normal dividing cells. Many previous studies have suggested that the additive or synergistic effects of the combined treatment of two or more drugs may be effective in chemotherapy (Emens and Middleton, 2015; Niedzwiecki *et al*., 2016). The approach to

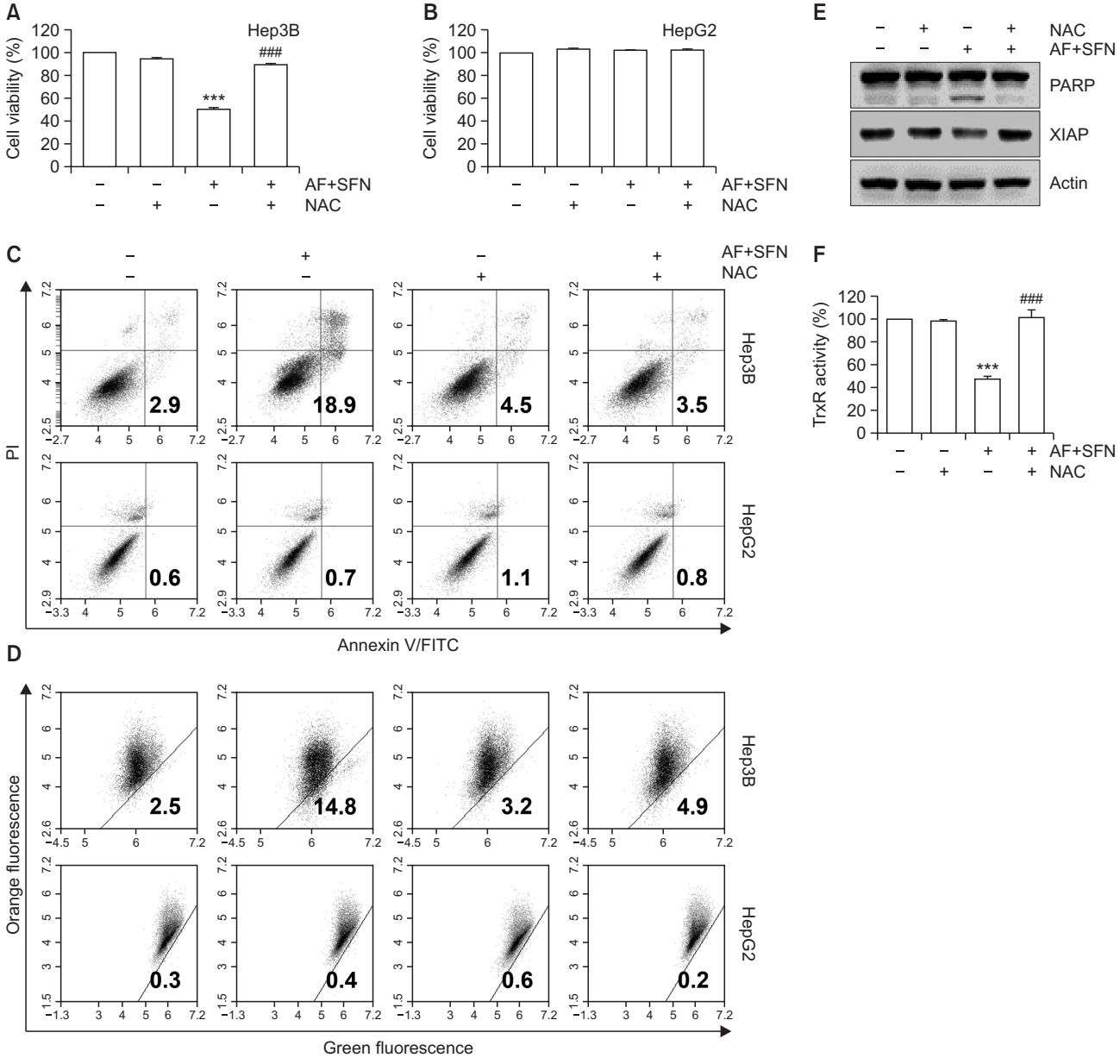

Fig. 7. The contribution of ROS production in apoptosis of Hep3B cells induced by combined treatment. The cells were pretreated with NAC for 1 h and then incubated with auranofin (AF) (1 μM) and sulforaphane (SFN) (7.5 μM) for 24 h. (A, B) Cell viability was determined by MTT assay. The error bars represent the standard deviation of three independent experiments. *** indicates significant differences at $p<0.001$, compared to the control group, ### indicates significant differences at $p<0.001$, compared to auranofin and sulforaphane-treated group. (C) Flow cytometry was carried out by annexin-V/PI staining to determine apoptosis. (D) A dot plot analysis of flow cytometry with JC-1 staining for the combined treatment with auranofin and sulforaphane compared to pretreatment with NAC. (E) The cells were lysed and equal amounts of cellular proteins were subjected to Western blotting analysis using specific primary antibodies corresponding to each protein. Equal protein loading was confirmed by actin expression. (F) TrxR activity was measured by DTNB reduction assay. Statistical analysis was performed using ANOVA with Tukey's post-hoc test. The error bars represent the standard deviation of three independent experiments. *** indicates significant differences at $p<0.001$, compared to the control group, ### indicates significant differences at $p<0.001$, compared to auranofin and sulforaphane-treated group.

combination therapy was conceived in the method of treating tuberculosis with antibiotic combinations in the 1960s and has been successfully achieved in the treatment of cancers such as acute lymphocytic leukemia and lymphoma (McKelvey *et al*., 1976; Robak *et al*., 2016; Kerantzas and Jacobs, 2017). Combination chemotherapy, which treats with drugs acting through molecular mechanisms, can reduce drug resistance and normal cell cytotoxicity by using two or more low-dose drugs instead of one high-dose drug while increasing cancer cell death (Pritchard *et al*., 2012).

TrxR is a pivotal enzyme that maintains or regulates the intracellular redox system and is highly sensitive to gold com-

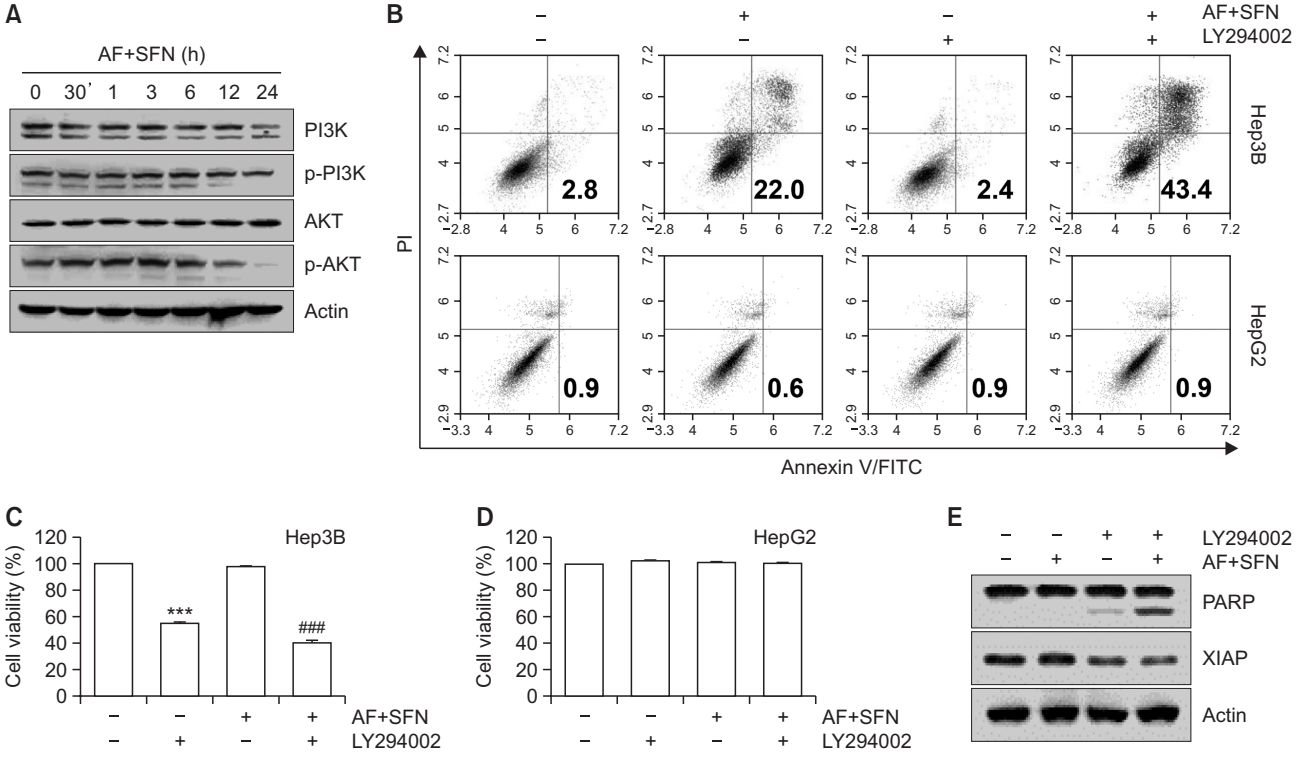

Fig. 8. Suppression of PI3K/Akt signaling pathway by the combined treatment in Hep3B cells. (A) The cells were treated with auranofin (AF) (1 μM) and sulforaphane (SFN) (7.5 μM) for the indicated time. For Western blot analysis, total cell lysates were separated by SDS-PAGE. After that, the proteins were blotted onto membranes and the specific antibodies were incubated to observe protein expression. Actin served as a control for equal loading. The cells were treated with LY294002 (5 μM) as a pharmacological inhibitor of PI3K/Akt 1 h prior to combined treatment with auranofin (1 μM) and sulforaphane (7.5 μM). After incubation for 24 h, apoptotic cell death was measured by annexin-V/PI staining using flow cytometry (B). (C, D) The cell viability was determined by MTT assay. The data are presented as the means ± SD of at least three independent experiments. *** indicates significant differences at $p<0.001$, compared to control group; ### indicates significant differences at $p<0.001$, compared to auranofin and sulforaphane-treated group. Apoptosis-related proteins were detected by Western blotting under the same conditions as above (E).

pounds including auranofin (Omata *et al*., 2006; Ouyang *et al*., 2018). The overexpression of TrxR has been selected as a defensive mechanism by external stimuli in various types of cancer cells (Jia *et al*., 2019). Hence, the dysfunction of TrxR or the inhibition of TrxR activity both represent novel strategies for human cancer therapy, and TrxR is emerging as a potential target for anti-cancer drug design. We predicted the possibility that auranofin and sulforaphane could bind to the active site of TrxR and investigated whether it could inhibit the activity of TrxR. According to the results of three-dimensional (3D) structural protein-chemical complex prediction, auranofin could bind to the active cysteine residue site of TrxR. Sulforaphane was weaker than auranofin but had the potential to combine with TrxR (Fig. 10). Binding with TrxR was confirmed to affect its activity, as expected. TrxR activity was decreased depending on the concentration of auranofin, whereas treatment with sulforaphane did not change the activity of TrxR. Interestingly, the TrxR activity measured following combined treatment was lower than that of the single treatments, exhibiting a synergistic effect (Fig. 2A-2C). In this study, combined treatment is proposed as a candidate for chemotherapy to effectively treat HCC. However, Hep3B cells were more sensitive to TrxR activity effects by sulforaphane and auranofin than HepG2 cells, indicating that the TrxR system played an important role in maintaining Hep3B cells as cancer cells.

In this study, auranofin or sulforaphane was treated separately under conditions that did not affect cell viability to maximize the effect of combination treatment. Combined treatment with auranofin and sulforaphane did not have a significant effect on normal hepatocytes, whereas, in Hep3B cells, the combination treatment synergistically decreased cell viability (Fig. 2). Combined treatment-induced cell death revealed features of apoptosis. The population of sub-G1 cells and the percentage of cells with annexin-V-positive staining, representing apoptosis, also increased (Fig. 3). The important proteins in the execution of apoptosis are caspases. Caspases acted differently in the apoptotic stages and are divided into initiator caspases, such as caspase-8 and -9, and effector caspases, including caspase-3 and -7 (Green and Llambi, 2015). Combined treatment activated caspase-9 and caspase-3, which increased the cleavage form of its substrate such as PARP. In contrast, the expression of XIAP and cIAP-1 was reduced by treatment with auranofin plus sulforaphane (Fig. 4). In addition, the combined treatment increased the expression of the mitochondrial permeabilization regulator Bax, and increased the Bax/Bcl-2 ratio even though the expression of Bcl-2 was unchanged. Since the activity and expression of caspase-8 and Bid were consistent compared to the controls, the extrinsic pathway was not associated with combined treatment-induced apoptosis. The alteration in the expression of

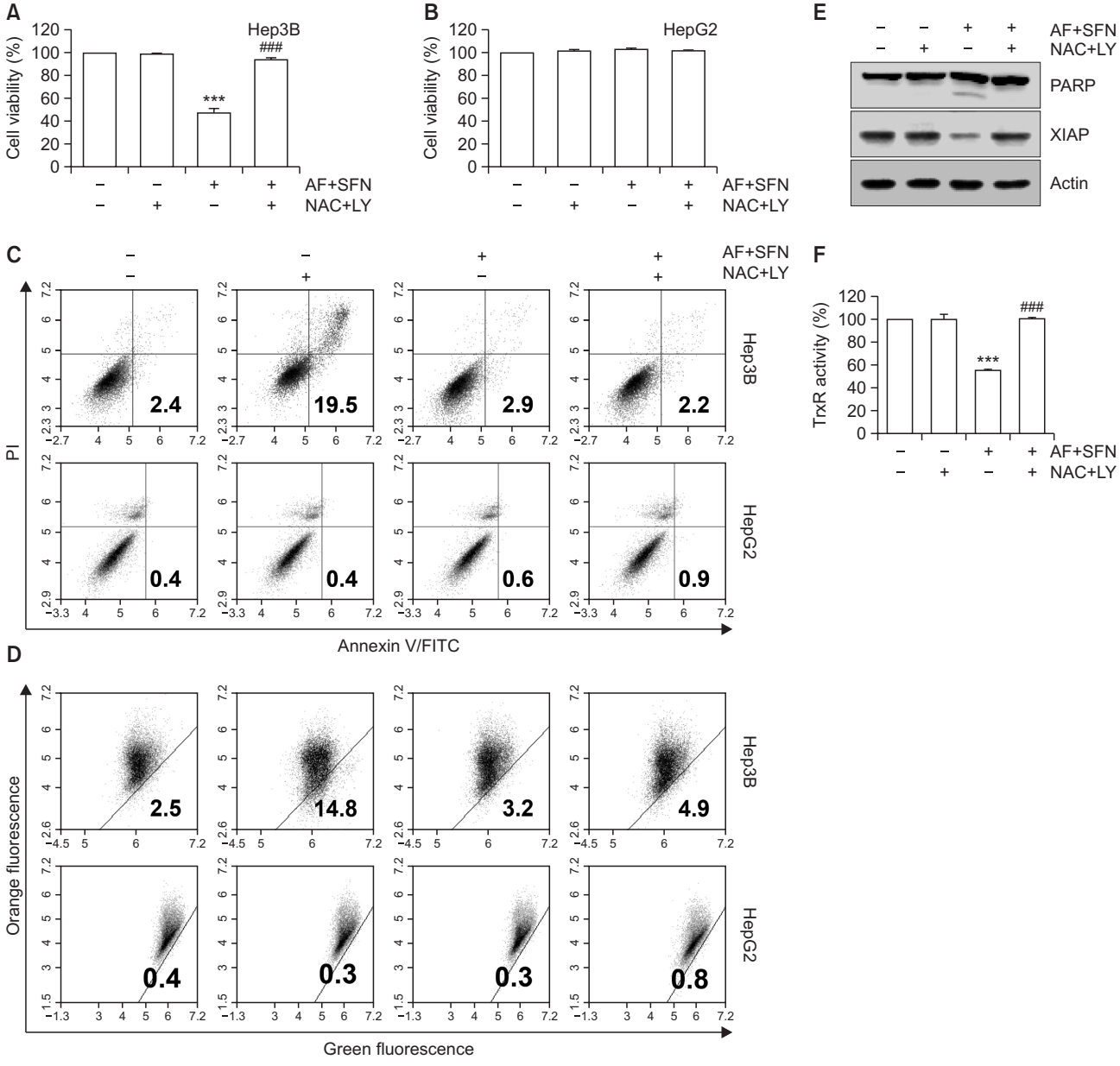

Fig. 9. ROS-mediated PI3K/Akt signaling pathway modulated combined treatment-induced apoptosis in Hep3B cells. The cells were pre-treated with NAC (10 mM) and LY294002 (5 μM) for 1 h prior to combined treatment with auranofin (AF) (1 μM) and sulforaphane (SFN) (7.5 μM). (A, B) Cell viability and TrxR activity were measured by MTT assay and DTNB reduction assay, respectively. The error bars represent the standard deviation of three independent experiments. *** indicates significant differences at $p<0.001$, compared to the control group; ### indicates significant differences at $p<0.001$, compared to auranofin and sulforaphane-treated group. (C) Following treatment, the cells were stained with annexin-V/PI and analyzed by flow cytometry. (D) MMP was measured by JC-1 staining and analyzed flow cytometry. (E) Alterations in apoptosis-related protein expression were analyzed by Western blotting. Total cell lysates were separated by SDS-PAGE, and the proteins were transferred to membranes. Each membrane was reacted with the indicated antibodies against apoptosis-related proteins. Actin served as a control for equal loading. (F) TrxR activity was measured by DTNB reduction assay. Statistical analysis was performed using ANOVA with Tukey's post-hoc test. The error bars represent the standard deviation of three independent experiments. *** indicates significant differences at $p<0.001$, compared to the control group, ### indicates significant differences at $p<0.001$, compared to auranofin and sulforaphane-treated group.

mitochondrial proteins by the combined treatment suggests mitochondria dysfunction. MMP ($\Delta\psi m$) plays an important role in mitochondrial homeostasis and is a driving force for the transport of ions and proteins required for mitochondrial function, which were reduced by the combined treatment (Zorova *et al*., 2018). Therefore, combined treatment-induced apoptosis may be a potential approach in inhibiting cancer by targeting mitochondria.

Apoptosis induced by oxidative stress is a much-discussed paradigm for the treatment strategy of cancer (Gerl and Vaux,

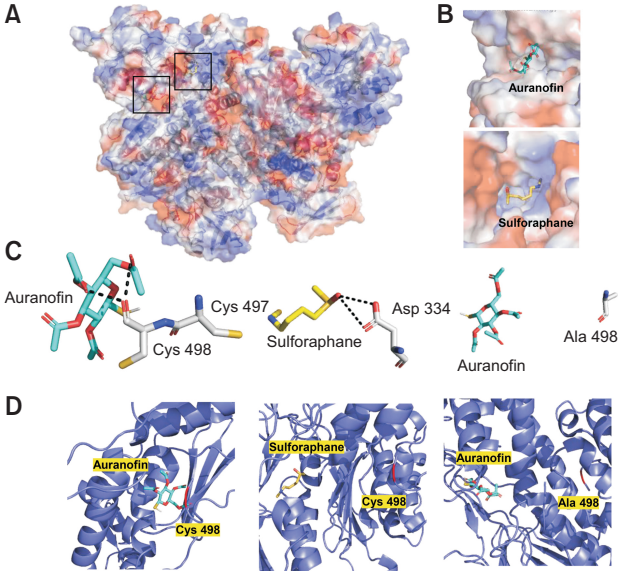

Fig. 10. Molecular docking of TrxR1 with auranofin and sulforaphane. (A) The interactions between TrxR1 (PDB identification (PDB ID): 2CFY) with auranofin (cyan stick) and sulforaphane (yellow stick) were calculated using PyRx and visualized by PyMOL. (B) The surface structure of TrxR1 binding auranofin and sulforaphane in the surface pocket, respectively (upper and bottom panels). (C) The covalent bond (black dotted line) formed between TrxR1 (Cys 498 and Asp 334 residue) and auranofin and sulforaphane, respectively (left and middle panel). The TrxR1 mutated to Ala 498 invalidated the interaction with auranofin (right panel). (D) Ribbon diagram for TrxR1 structure with auranofin and sulforaphane. The Cys 498 residue is shown in red color in the left and middle panels, and the Ala 498 residue is shown in red in the right panel.

2005). In particular, combined treatment inhibited the activity of TrxR, a component of the oxidative defense system, and promoted the generation of ROS (Fig. 6, 7). In this case, DCFH-DA staining of intracellular ROS and mitochondrial indicator were observed to be co-localized. Additionally, the occurrence of mitochondrial superoxide was measured by MitoSOX, and the results showed that auranofin and sulforaphane treatment increased MitoSOX-stained cells. However, the inhibition of TrxR activity and cell viability by the combined treatment was restored by a free radical scavenger (NAC). Moreover, apoptotic cell death and the loss of MMP were recovered by NAC pretreatment, resulting in a reduction of cleaved PARP and an increase of XIAP. Consequently, mitochondrial-mediated ROS was induced by the combined treatment, and the generated ROS regulated auranofin and sulforaphane-induced apoptosis.

Activation of PI3K/Akt signaling pathway is a representative anticancer target in types of cancers because it can regulate various cellular functions, including cell proliferation, inhibition of apoptosis, tumor growth and angiogenesis (Yu and Cui, 2016; Cheng *et al*., 2019). Considering that PI3K/Akt signaling plays an important role in cancer cells, whether combined treatment influenced the expression and phosphorylation of PI3K and Akt was investigated. The expression of p-PI3K and p-Akt was decreased by treatment with auranofin plus sulforaphane in a time-dependent manner, suggesting that PI3K/Akt signaling pathway should be considered in auranofin and sulforaphane-induced apoptosis. Furthermore, pretreatment with a PI3K inhibitor (LY294002) confirmed the alteration in combined treatment-induced apoptosis. Pretreatment with the PI3K inhibitor induced more cell death than the combined treatment, indicating that the apoptosis induced by auranofin and sulforaphane was due to inhibition of PI3K/Akt signaling pathway. Because the time of ROS occurrence was earlier than inhibition of the PI3K/Akt pathway, the generation of ROS was expected to act upstream in combined treatment-induced apoptosis. To confirm whether ROS and PI3K/Akt signaling pathway were independent or related to each other, an ROS scavenger and PI3K inhibitor were used to pretreat Hep3B cells. As shown in Fig. 9, despite the presence of PI3K inhibitor, cell viability and TrxR activity were recovered by NAC pretreatment, and apoptotic cell death and loss of MMP decreased. Thus, combined treatment induced apoptosis, inhibiting the PI3K/Akt signaling pathway dependent upon ROS generation.

These results demonstrated that auranofin and sulforaphane could synergistically induce apoptosis in Hep3B cells, and the combined treatment enhanced mitochondrial dysfunction and ROS accumulation and decreased decreasing TrxR activity in the process of inducing apoptosis.

ACKNOWLEDGMENTS

This research was funded by Basic Science Research Program through the National Research Foundation of Korea (NRF) grant funded by the Korea government (2018R1A2B2005705), Republic of Korea.

REFERENCES

Arnér, E. S. and Holmgren, A. (2000) Physiological functions of thioredoxin and thioredoxin reductase. *Eur. J. Biochem.* **267**, 6102-6109.

Baffy, G., Brunt, E. M. and Caldwell, S. H. (2012) Hepatocellular carcinoma in non-alcoholic fatty liver disease: an emerging menace. *J. Hepatol.* **56**, 1384-1391.

Becker, K., Gromer, S., Schirmer, R. H. and Müller, S. (2000) Thioredoxin reductase as a pathophysiological factor and drug target. *Eur. J. Biochem.* **267**, 6118-6125.

Cheng, S., Zhang, X., Feng, Q., Chen, J., Shen, L., Yu, P., Yang, L., Chen, D., Zhang, H., Sun, W. and Chen, X. (2019) Astragaloside IV exerts angiogenesis and cardioprotection after myocardial infarction via regulating PTEN/PI3K/Akt signaling pathway. *Life Sci.* **227**, 82-93.

Cheng, Y. and Qi, Y. (2017) Current progresses in metal-based anticancer complexes as mammalian TrxR inhibitors. *Anticancer Agents Med. Chem.* **17**, 1046-1069.

Conklin, K. A. (2000) Dietary antioxidants during cancer chemotherapy: impact on chemotherapeutic effectiveness and development of side effects. *Nutr. Cancer* **37**, 1-18.

Cox, A. G., Brown, K. K., Arner, E. S. and Hampton, M. B. (2008) The thioredoxin reductase inhibitor auranofin triggers apoptosis through a Bax/Bak-dependent process that involves peroxiredoxin 3 oxidation. *Biochem. Pharmacol.* **76**, 1097-1109.

Emens, L. A. and Middleton, G. (2015) The interplay of immunotherapy and chemotherapy: harnessing potential synergies. *Cancer Immunol. Res.* **3**, 436-443.

Fang, J. and Holmgren, A. (2006) Inhibition of thioredoxin and thioredoxin reductase by 4-hydroxy-2-nonenal *in vitro* and *in vivo*. *J. Am. Chem. Soc.* **128**, 1879-1885.

Ferlay, J., Ervik, M., Lam, F., Colombet, M., Mery, L., Piñeros, M., Znaor, A., Soerjomataram, I. and Bray, F. (2018) Global Cancer

Observatory: Cancer Today. International Agency for Research on Cancer, Lyon. Available from: https://gco.iarc.fr/today/ [accessed 2019 Mar 25].

Gamet-Payrastre, L., Li, P., Lumeau, S., Cassar, G., Dupont, M. A., Chevolleau, S., Gasc, N., Tulliez, J. and Tercé, F. (2000) Sulforaphane, a naturally occurring isothiocyanate, induces cell cycle arrest and apoptosis in HT29 human colon cancer cells. *Cancer Res.* **60**, 1426-1433.

Gerl, R. and Vaux, D. L. (2005) Apoptosis in the development and treatment of cancer. *Carcinogenesis* **26**, 263-270.

Green, D. R. and Llambi, F. (2015) Cell death signaling. *Cold Spring Harb. Perspect. Biol.* **7**, a006080.

Hasan, M. M., Islam, M. S., Hoque, K. M. F., Haque, A. and Reza, M. A. (2019) Effect of Citrus macroptera fruit pulp juice on alteration of caspase pathway rendering anti-proliferative activity against Ehrlich's ascites carcinoma in mice. *Toxicol. Res.* **35**, 271-277.

Herman-Antosiewicz, A., Johnson, D. E. and Singh, S. V. (2006) Sulforaphane causes autophagy to inhibit release of cytochrome C and apoptosis in human prostate cancer cells. *Cancer Res.* **66**, 5828-5835.

Hwang-Bo, H., Jeong, J. W., Han, M. H., Park, C., Hong, S. H., Kim, G. Y., Moon, S. K., Cheong, J., Kim, W. J., Yoo, Y. H. and Choi, Y. H. (2017) Auranofin, an inhibitor of thioredoxin reductase, induces apoptosis in hepatocellular carcinoma Hep3B cells by generation of reactive oxygen species. *Gen. Physiol. Biophys.* **36**, 117-128.

Hwang-Bo, H., Lee, W. S., Nagappan, A., Kim, H. J., Panchanathan, R., Park, C., Chang, S. H., Kim, N. D., Leem, S. H., Chang, Y. C., Kwon, T. K., Cheong, J. H., Kim, G. S., Jung, J. M., Shin, S. C., Hong, S. C. and Choi, Y. H. (2019) Morin enhances auranofin anticancer activity by up-regulation of DR4 and DR5 and modulation of Bcl-2 through reactive oxygen species generation in Hep3B human hepatocellular carcinoma cells. *Phytother. Res.* **33**, 1384-1393.

Isab, A. A. and Shaw, C. F., 3rd (1990) Synthesis of thionato(triethylphosphine) gold(I) complexes: analogues of "auranofin" an antiarthritic drug. *J. Inorg. Biochem.* **38**, 95-100.

Jia, J. J., Geng, W. S., Wang, Z. Q., Chen, L. and Zeng, X. S. (2019) The role of thioredoxin system in cancer: strategy for cancer therapy. *Cancer Chemother. Pharmacol.* **84**, 453-470.

Kerantzas, C. A. and Jacobs, W. R., Jr. (2017) Origins of combination therapy for tuberculosis: lessons for future antimicrobial development and application. *mBio* **8**, e01586-16.

Kulik, L. and El-Serag, H. B. (2019) Epidemiology and management of hepatocellular carcinoma. *Gastroenterology* **156**, 477-491.

Li, Y., Zhang, T., Korkaya, H., Liu, S., Lee, H. F., Newman, B., Yu, Y., Clouthier, S. G., Schwartz, S. J., Wicha, M. S. and Sun, D. (2010) Sulforaphane, a dietary component of broccoli/broccoli sprouts, inhibits breast cancer stem cells. *Clin. Cancer Res.* **16**, 2580-2590.

Likhitsup, A., Razumilava, N. and Parikh, N. D. (2019) Treatment for advanced hepatocellular carcinoma: current standard and the future. *Clin. Liver Dis. (Hoboken)* **13**, 13-19.

Lincoln, D. T., Ali, Emadi, E. M., Tonissen, K. F. and Clarke, F. M. (2003) The thioredoxin-thioredoxin reductase system: over-expression in human cancer. *Anticancer Res.* **23**, 2425-2433.

Llovet, J. M., Montal, R., Sia, D. and Finn, R. S. (2018) Molecular therapies and precision medicine for hepatocellular carcinoma. *Nat. Rev. Clin. Oncol.* **15**, 599-616.

Lu, J. and Holmgren, A. (2014) The thioredoxin antioxidant system. *Free. Radic. Biol. Med.* **66**, 75-87.

Madeira, J. M., Gibson, D. L., Kean, W. F. and Klegeris, A. (2012) The biological activity of auranofin: implications for novel treatment of diseases. *Inflammopharmacology* **20**, 297-306.

Marzano, C., Gandin, V., Folda, A., Scutari, G., Bindoli, A. and Rigobello, M. P. (2007) Inhibition of thioredoxin reductase by auranofin induces apoptosis in cisplatin-resistant human ovarian cancer cells. *Free Radic. Biol. Med.* **42**, 872-881.

McKelvey, E. M., Gottlieb, J. A., Wilson, H. E., Haut, A., Talley, R. W., Stephens, R., Lane, M., Gamble, J. F., Jones, S. E., Grozea, P. N., Gutterman, J., Coltman, C. and Moon, T. E. (1976) Hydroxyldaunomycin (Adriamycin) combination chemotherapy in malignant lymphoma. *Cancer* **38**, 1484-1493.

Mi, L., Wang, X., Govind, S., Hood, B. L., Veenstra, T. D., Conrads, T. P., Saha, D. T., Goldman, R. and Chung, F. L. (2007) The role of protein binding in induction of apoptosis by phenethyl isothiocyanate and sulforaphane in human non-small lung cancer cells. *Cancer Res.* **67**, 6409-6416.

Moon, D. O., Kang, S. H., Kim, K. C., Kim, M. O., Choi, Y. H. and Kim, G. Y. (2010) Sulforaphane decreases viability and telomerase activity in hepatocellular carcinoma Hep3B cells through the reactive oxygen species-dependent pathway. *Cancer Lett.* **295**, 260-266.

Niedzwiecki, A., Roomi, M. W., Kalinovsky, T. and Rath, M. (2016) Anticancer efficacy of polyphenols and their combinations. *Nutrients* **8**, 552.

Omata, Y., Folan, M., Shaw, M., Messer, R. L., Lockwood, P. E., Hobbs, D., Bouillaguet, S., Sano, H., Lewis, J. B. and Wataha, J. C. (2006) Sublethal concentrations of diverse gold compounds inhibit mammalian cytosolic thioredoxin reductase (TrxR1). *Toxicol. In Vitro* **20**, 882-890.

Ouyang, Y., Peng, Y., Li, J., Holmgren, A. and Lu, J. (2018) Modulation of thiol-dependent redox system by metal ions via thioredoxin and glutaredoxin systems. *Metallomics* **10**, 218-228.

Phan, M. A. T., Paterson, J., Bucknall, M. and Arcot, J. (2018) Interactions between phytochemicals from fruits and vegetables: effects on bioactivities and bioavailability. *Crit. Rev. Food Sci. Nutr.* **58**, 1310-1329.

Pritchard, J. R., Lauffenburger, D. A. and Hemann, M. T. (2012) Understanding resistance to combination chemotherapy. *Drug Resist. Updat.* **15**, 249-257.

Ralph, S. J., Nozuhur, S., ALHulais, R. A., Rodríguez-Enríquez, S. and Moreno-Sánchez, R. (2019) Repurposing drugs as pro-oxidant redox modifiers to eliminate cancer stem cells and improve the treatment of advanced stage cancers. *Med. Res. Rev.* **39**, 2397-2426.

Ren, X., Zou, L., Lu, J. and Holmgren, A. (2018) Selenocysteine in mammalian thioredoxin reductase and application of ebselen as a therapeutic. *Free Radic. Biol. Med.* **127**, 238-247.

Robak, T., Blonski, J. Z. and Robak, P. (2016) Antibody therapy alone and in combination with targeted drugs in chronic lymphocytic leukemia. *Semin. Oncol.* **43**, 280-290.

Robbins, R. J., Keck, A. S., Banuelos, G. and Finley, J. W. (2005) Cultivation conditions and selenium fertilization alter the phenolic profile, glucosinolate, and sulforaphane content of broccoli. *J. Med. Food* **8**, 204-214.

Schirrmacher, V. (2019) From chemotherapy to biological therapy: a review of novel concepts to reduce the side effects of systemic cancer treatment (review). *Int. J. Oncol.* **54**, 407-419.

Trotti, A., Byhardt, R., Stetz, J., Gwede, C., Corn, B., Fu, K., Gunderson, L., McCormick, B., Morrisintegral, M., Rich, T., Shipley, W. and Curran, W. (2000) Common toxicity criteria: version 2.0. an improved reference for grading the acute effects of cancer treatment: impact on radiotherapy. *Int. J. Radiat. Oncol. Biol. Phys.* **47**, 13-47.

Urig, S. and Becker, K. (2006) On the potential of thioredoxin reductase inhibitors for cancer therapy. *Semin. Cancer Biol.* **16**, 452-465.

U.S. National Library of Medicine, ClinicalTrials.gov. Available from: https://clinicaltrials.gov/ct2/home/.

Yu, J. S. and Cui, W. (2016) Proliferation, survival and metabolism: the role of PI3K/AKT/mTOR signalling in pluripotency and cell fate determination. *Development* **143**, 3050-3060.

Zhang, N., Li, F., Gao, J., Zhang, S. and Wang, Q. (2020) Osteopontin accelerates the development and metastasis of bladder cancer via activating JAK1/STAT1 pathway. *Genes Genomics* **42**, 467-475.

Zhong, L., Arnér, E. S. and Holmgren, A. (2000) Structure and mechanism of mammalian thioredoxin reductase: the active site is a redox-active selenolthiol/selenenylsulfide formed from the conserved cysteine-selenocysteine sequence. *Proc. Natl. Acad. Sci. U.S.A.* **97**, 5854-5859.

Zorova, L. D., Popkov, V. A., Plotnikov, E. Y., Silachev, D. N., Pevzner, I. B., Jankauskas, S. S., Babenko, V. A., Zorov, S. D., Balakireva, A. V., Juhaszova, M., Sollott, S. J. and Zorov, D. B. (2018) Mitochondrial membrane potential. *Anal. Biochem.* **552**, 50-59.